



Characteristic sizes of life in the oceans - from bacteria to whales

Andersen, Ken Haste; Berge, T.; Goncalves, R.; Hartvig, Martin; Heuschele, Jan; Hylander, Samuel; Jacobsen, Nis Sand; Lindemann, Christian; Martens, Erik Andreas; Neuheimer, Anna

Total number of authors:
18

Published in:
Annual Review of Marine Science

Link to article, DOI:
[10.1146/annurev-marine-122414-034144](https://doi.org/10.1146/annurev-marine-122414-034144)

Publication date:
2016

Document Version
Peer reviewed version

[Link back to DTU Orbit](#)

Citation (APA):
Andersen, K. H., Berge, T., Goncalves, R., Hartvig, M., Heuschele, J., Hylander, S., Jacobsen, N. S., Lindemann, C., Martens, E. A., Neuheimer, A., Olsson, K., Palacz, A., Prowe, F., Sainmont, J., Traving, S. J., Visser, A., Wadhwa, N., & Kiørboe, T. (2016). Characteristic sizes of life in the oceans - from bacteria to whales. *Annual Review of Marine Science*, 8(3), 217-241. <https://doi.org/10.1146/annurev-marine-122414-034144>

General rights

Copyright and moral rights for the publications made accessible in the public portal are retained by the authors and/or other copyright owners and it is a condition of accessing publications that users recognise and abide by the legal requirements associated with these rights.

- Users may download and print one copy of any publication from the public portal for the purpose of private study or research.
- You may not further distribute the material or use it for any profit-making activity or commercial gain
- You may freely distribute the URL identifying the publication in the public portal

If you believe that this document breaches copyright please contact us providing details, and we will remove access to the work immediately and investigate your claim.

1 **Characteristic sizes of life in the oceans, from bacteria to**
2 **whales**

3 *Running title: Characteristic sizes of life in the oceans*

4

5 K.H. Andersen, T. Berge, R. J. Gonçalves, M. Hartvig, J. Heuschele, S. Hylander, N.S.
6 Jacobsen, C. Lindemann, E.A. Martens, A.B. Neuheimer, K. Olsson, A. Palacz, F.
7 Prowe, J. Sainmont, S.J. Traving, A.W. Visser, N. Wadhwa, and T. Kiørboe

8

9

10 K.H. Andersen^{1,2}: kha@aqua.dtu.dk. Corresponding author, tel. +45 35 88 33 99.

11 T. Berge^{1,8}: tberge@bio.ku.dk

12 R. J. Gonçalves^{1,2,10}: rgon@aqua.dtu.dk

13 M. Hartvig^{2,3,4}: mh@hvig.dk

14 J. Heuschele^{1,2}: janheuschele@gmail.com

15 S. Hylander^{2,9}: samuel.hylander@lnu.se

16 N.S. Jacobsen^{1,2}: nsja@aqua.dtu.dk

17 C. Lindemann^{1,2}: chrli@aqua.dtu.dk

18 E.A. Martens^{1,2,7}: erik.martens@ds.mpg.de

19 A.B. Neuheimer^{2,3,6}: annabn@hawaii.edu

20 K. Olsson^{1,2}: karol@aqua.dtu.dk

21 A. Palacz^{1,2}: arpa@aqua.dtu.dk

22 F. Prowe^{1,2,11}: fprowe@geomar.de

23 J. Sainmont^{1,2}: jusa@aqua.dtu.dk

24 S.J. Traving^{1,8}: sjtraving@bio.ku.dk

25 A.W. Visser^{1,2}: awv@aqua.dtu.dk

26 N. Wadhwa^{1,5}: nawa@fysik.dtu.dk

27 T. Kiørboe^{1,2}: tk@aqua.dtu.dk

28

29 1: VKR Centre for Ocean Life.

30 2: National Institute of Aquatic Resources, Technical University of Denmark,
31 Charlottenlund Slot, Jægersborg Allé, DK-2920 Charlottenlund, Denmark

32 3: Center for Macroecology, Evolution and Climate, Natural History Museum of
33 Denmark, University of Copenhagen, Universitetsparken 15, 2100 Copenhagen,
34 Denmark

35 4: Systemic Conservation Biology, J.F. Blumenbach Institute of Zoology and
36 Anthropology, University of Göttingen, Berliner Strasse 28, 37073 Göttingen,
37 Germany

38 5: Department of Physics, Technical University of Denmark

39 6: Department of Oceanography, University of Hawai'i at Mānoa, 1000 Pope
40 Road, Marine Sciences Building, Honolulu, HI 96822, USA.

41 7: Department of Biomedical Sciences, Copenhagen University, Blegdamsvej 3,
42 2200 Copenhagen, Denmark

43 8: Marine Biological Section, University of Copenhagen, Strandpromenaden 5,
44 3000 Helsingør, Denmark

45 9: Faculty of Health and Life Sciences, Linnaeus University, Kalmar, Sweden

46 10: Consejo Nacional de Investigaciones Científicas y Técnicas, Argentina

47 11: GEOMAR Helmholtz Centre for Ocean Research Kiel, Wischhofstr. 1-3,
48 24148 Kiel, Germany

49	Introduction	6
50	What is 'size'?	9
51	Resource acquisition and trophic strategies	10
52	Mobility	17
53	Size and sensing	19
54	Life history and progeny size	26
55	Transitions between life forms	28
56	Beyond size	35
57	Acknowledgements	37
58	Literature cited	37
59	Acronyms and definitions	46

60

61 *Keywords:* body size, metabolism, allometric scaling, plankton, mixotrophy, fish,
62 whales

63

64 The size of an individual organism is a key trait to characterize its physiology
65 and feeding ecology. Size-based scaling laws may have a limited size range of
66 validity or undergo a transition from one scaling exponent to another at some
67 characteristic size. We collate and review data on size-based scaling laws for
68 resource acquisition, mobility, sensory range and progeny size for all pelagic
69 marine life, from bacteria to whales. Further, we review and develop simple
70 theoretical arguments for observed scaling laws and the characteristic sizes of a

71 change or breakdown of power laws. We divide life in the ocean into seven major
72 realms based on their trophic strategy, physiology and life history strategy. Such
73 a categorization represents a move away from a taxonomically oriented
74 description towards a trait-based description of life in the oceans. Finally, we
75 discuss life forms that transgress the simple size-based rules and identify
76 unanswered questions.

77

78 *Number of words in abstract: 149*

79 *Number of words in text: 7500*

80 *Number of words in Sidebar 1: 542*

81 *Number of words in Sidebar 2: 375*

82 *Number of references: 93 (limit 100).*

83 *Number of figures, tables and text-boxes: 7, 1, 2 (limit 10)*

84 *Online appendices: 4.*

Introduction

Since the essay by Haldane (1928) “On being the right size” biologists have used organism size as a master trait to characterize the capabilities and limitations of individual organisms. There are good reasons for doing so. It is evident that the physiology and ecology of a copepod and a dolphin are vastly different, much more so than the difference between a copepod and a fish larva. Organism size describes individual physiology across major taxa through power-law functions (Peters 1983): metabolism, leading to the celebrated 3/4 law for the scaling of resting metabolism with size (Hemmingsen 1960, Kleiber 1932, West et al. 1997, Winberg 1956), population growth rates (Fenchel 1974, Gillooly et al. 2002), predator-prey relationships in terms of functional response (Hansen *et al.* 1997; Kiørboe 2011; Rall *et al.* 2012) and predator-prey ratios (Barnes et al. 2008, Cohen et al. 1993, Hansen et al. 1994), fluid-mechanical forces (Bejan & Marden 2006), swimming speed (Ware 1978; Kiørboe 2011), vision (Dunbrack & Ware 1987), diffusive uptake affinities (Aksnes & Egge 1991, Berg & Purcell 1977, Edwards et al. 2012, Litchman et al. 2007, Munk & Riley 1952, Tambi et al. 2009) and, for phytoplankton, affinities for light (Finkel 2001, Taguchi 1976) and maximum uptake rates (Edwards et al. 2012, Marañón et al. 2013). Size has also been used to describe macro-ecological patterns of size-dependent species diversity (Fenchel & Finlay 2004, May 1975, Reuman et al. 2014), and the biomass distribution of individuals as a function of size across major taxa (Boudreau & Dickie 1992, Sheldon & Prakash 1972) has been explained theoretically using the size relationships describing individual physiology (Sheldon *et al.* 1977; Andersen & Beyer 2006). While developing these size-

based relations the focus has been on determining the exponent (the “slope”) and the constant (“intercept”), with less attention being paid to the sizes that limits the range of their validity.

On closer inspection, some power-laws relationships are seen to change scaling exponent and/or intercept around some particular size or even break down altogether beyond a range of validity. The fluid flow around a whale, for example, is turbulent leading to dominance of inertial forces with a drag force scaling with the length and velocity squared. In contrast, the flow around a unicellular organism is laminar and dominated by viscous forces with a drag force scaling linearly with velocity and length. Consequently, the scaling of drag force changes at the organism size where there is a transition between viscous and turbulent flow. As example of a breakdown, consider the visual range. The larger the eye, the longer an organism can see. However, there is an upper visual range determined by the sensitivity of the retina (Dunbrack & Ware 1987), as well as a lower limit of eye size determined by the size of the visual elements in the retina and the wavelength of light. The scaling law for visual range is therefore valid only within the upper and lower limits. Such changes or breakdowns in scaling laws have consequences for adaptations and strategies of marine organisms. For example, predators so large that they are in the inertial fluid regime develop a streamlined body shape for efficient swimming and predators smaller than the lower size of an eye cannot rely on vision.

Haldane (1928) concluded that *“For every type of animal there is a most convenient size, and a large change in size inevitably carries with it a change of form”*. Our aim is to determine the sizes where scaling relationships change or break down and to use those characteristic sizes to explain the fundamental differences in the form and function of marine organisms with different sizes. To this end we build on the large existing literature of empirical size-based scaling relations and their theoretic explanations.

We categorize pelagic life in the ocean based on size in seven general realms: molecular life (viruses), osmo-heterotrophic bacteria, unicellular phototrophs, unicellular mixotrophs and heterotrophs, planktonic multi-cellular heterotrophs (e.g. copepods), visually foraging poikilotherms (e.g. fish), and homeothermic animals (whales). This categorization of life is a deliberately crude representation of the roughly 200,000 eukaryotic species, plus an unknown number of archaea and bacteria, in the ocean (May & Godfrey 1994), as it is explicitly designed to facilitate an understanding based on size. We describe the life forms in each realm according to their body size and determine characteristic sizes where there is a transition from one realm to another. In this manner we emphasize body size as a fundamental driver of macro-ecological patterns in the oceans.

We examine five aspects of life where size is a dominant driver: (i) resource encounter through predation, diffusive uptake or photosynthesis, (ii) mobility, (iii) sensing through chemical and hydromechanical signals, vision, and

echolocation, (iv) life history strategy in terms of adult and progeny sizes and (v) body temperature (Figure 1). To this end we draw on a wide range of theories: diffusion theory, fluid mechanics, optics, metabolic theory, and optimal life history theory. We review established theoretical and empirical scaling laws and establish characteristic sizes where the scaling laws change or break down. These characteristic sizes are used to formulate hypotheses about the dominant strategy for organisms of a given size within the five aspects, e.g. how an organism obtains carbon (through photosynthetic assimilation of inorganic carbon, from dissolved organic matter, or from particulate organic matter), or which senses it employs for prey encounter. We test the hypotheses by collecting data on strategies of individuals as a function of their size. Since our arguments are general in nature they apply largely to all aquatic life but our focus is pelagic marine life. The final synthesis is a description of the dominant forms and functions of life in the oceans. This is used to frame a discussion of strategies and life forms that transcends the general size-based patterns and to point towards open unanswered questions.

What is 'size'?

The size of an organism can be characterized by its length or by its weight. Wet weight, dry weight and carbon weight are the most common weight measures, while length is typically measured as the largest linear dimension or the equivalent spherical diameter (ESD). Depending on the question one measure may be more appropriate than the other. For example the flow around an organism is determined by its linear size and shape, not by its weight. Conversely, the bioenergetic budget of an organism is adequately described in

terms of weight since the energetic budget should reflect a conservation of mass. For microbes weight is often measured in carbon or in units of the limiting nutrients since water content and ratios between fundamental elements vary between organisms (Klausmeier et al. 2004). The elemental ratios and water content of vertebrates vary less than they do for invertebrates so wet weight is often preferred as an intuitive measure of weight for vertebrates. Even though it would be possible, we do not find it useful to convert all sizes to a common measure and consequently use the most convenient measure depending on the situation. We will use the symbols w for a weight and l for length, d for diameter and r for radius and frequently make use of the conversion between length and weight as $w \propto l^3$. Units of weight are indicated with subscripts: g_{WW} , g_C , referring to wet weight and carbon weight. Conversion relations are provided in Table S1.1.

Resource acquisition and trophic strategies

Organisms acquire carbon and nutrients through feeding on encountered resources. “Resources” is here understood broadly as dissolved inorganic nutrients, dissolved organic molecules, photons or prey organisms. The encounter with resources occurs by three mechanisms: 1) active encounter through cruising, ambushing or creation of a feeding current, 2) fixation of carbon through photosynthesis or, 3) passive encounter with food items which diffuse towards the feeding individual. The encounter rate (biomass per time) is described as:

$$E = \beta C \quad (1)$$

203

204 where β is the clearance rate (volume per time) and C the resource
 205 concentration (biomass per volume). In terms of a type II functional response
 206 (Holling 1959) the clearance rate is the slope at the origin i.e., the potential
 207 volume of water cleared for resources per unit time when uptake is not limited
 208 by handling time or physiological limits (digestion). These limitations are not
 209 considered here. The clearance rate is described as a power function of size
 210 $\beta = bl^a$. We employ the linear dimension l to characterize size because resource
 211 uptake is determined by the physical size of an organism, not by its weight. In the
 212 following we describe how the exponent a and the factor b depends on size for
 213 the three different resource acquisition mechanisms on the basis of physical
 214 processes and empirical cross-species relationships. This analysis allows us to
 215 characterize the dominant trophic strategy of organisms, e.g. phototrophs or
 216 heterotrophs, as a function of their size and the biotic and abiotic environment.

217

218 *Active predation*

219 Large protozoans and metazoans have three fundamental modes of actively
 220 encountering prey: ambushing, generating a feeding current or cruising through
 221 the water searching for prey (Kiørboe, 2011). The clearance rate of each mode
 222 β_A can be estimated as a velocity multiplied by an encounter cross section. A
 223 planktonic filter-feeder, for example, captures prey on its filter with a size scaling
 224 as the length of the organism squared l^2 , with a feeding-current velocity $u \approx l^{0.8}$
 225 (Huntley & Zhou 2004) leading to a scaling exponent of the clearance rate of

$a_A \approx 2.8$. Using similar arguments for the other feeding modes all lead to exponents ≈ 2.8 , i.e. slightly below 3, but multiplied by different factors (Kjørboe 2011). Since one feeding mode replaces the other depending on environmental conditions and the size of the prey and the predator, the average life-form-transcending scaling exponent becomes around 3 (Figure 2a; Table S1.2):

$$\beta_A = b_A l^3$$

Weight-specific uptakes rates, $\propto \beta_A/w$, are therefore independent of size since $w \propto l^3$ (Kjørboe & Hirst 2014).

Photosynthesis

Fixation of dissolved CO_2 by photosynthesis requires encounter with photons (we assume that CO_2 is not limiting). Photosynthesis can in principle occur throughout the cell but for larger cells it is limited by self-shading of photons (the “package effect”) (Morel & Bricaud 1981). For the present arguments, it is sufficient to consider that the cross-sectional area of the cell $\propto l^2$ limits photosynthesis (Figure 2b):

$$\beta_L = b_L l^2 \quad (2).$$

The clearance rate β_L is often termed light affinity or photosynthetic efficiency and is measured in dimensions of carbon fixed per photon multiplied by area. In terms of weight specific scaling, the power 2 scaling of β_L results in a scaling of weight specific rates of carbon fixation $\beta_L/w \propto w^{-1/3}$, i.e. smaller organisms have a higher specific rate of carbon fixation than larger ones. Organisms smaller than a certain size are therefore able to fix more carbon by photosynthesis than by active encounter since specific uptake by active encounter is independent of size.

Diffusion feeding

Organisms that encounter resource items as they bump into the surface of the organism due to Brownian motion are termed “diffusion feeding” (Fenchel 1984). Diffusion feeding is used to assimilate dissolved organic molecules, inorganic carbon and nutrients. The uptake rate is limited by the number of uptake sites on the surface of the cell, which can be expected to scale with l^2 . However, the uptake also removes resources from the vicinity of the cell surface and creates a boundary layer of lower resource concentrations near the cell than far away (Munk & Riley 1952). This effectively leads to the clearance rate β_D being limited rather by diffusion than by the surface, with a scaling proportional to the linear dimension of the cell (reviewed by Fiksen et al. 2013):

$$\beta_D = b_D l^1 \quad (3).$$

Weight specific uptake rates are then $\propto w^{-2/3}$, i.e., high for small cells and declining with size. Small diffusion feeding cells therefore have a higher encounter rate with dissolved nutrients or macromolecules than they could have obtained by active feeding. The theoretic scaling prediction fits with data for phosphate affinity (Figure 2c). Data for nitrogen affinity are less clear, with some being consistent with the theoretic scaling ($a_D = 1.2$) (Litchman et al. 2007) and others not ($a_D = 2.25$) (Edwards et al. 2012).

Trophic strategies

An organism's trophic strategy, i.e., which type of food it consumes, is to a large degree determined by its resource acquisition mechanism. It can be an osmotroph that diffusion feeds on dissolved organic matter (bacteria), a phototroph that captures light and diffusion feeds on dissolved inorganic nutrients (phytoplankton), a mixotroph that captures light and feeds on other organisms, or an actively feeding heterotroph (animals and many protists). If we use clearance rate as a proxy for competitive ability at low resource concentrations, we can assume that the dominant trophic strategy of organisms at a given size is determined by the resource acquisition mechanism yielding the highest encounter rate. The encounter rates for the four trophic strategies as a function of size is given by Eq. 1 where the resource may be either concentrations of dissolved organic molecules C_{DOM} , nutrients C_N , other prey organisms C_P , or the light flux C_L . Phototrophs need special treatment since they assimilate inorganic carbon and nutrients by two different processes. Carbon is

assimilated through photosynthesis and combined with diffusively encountered nutrients to achieve a C/N ratio c_{CN} . The limiting compound determines encounter as described by Liebig's law of the minima:

$$E = \min\{c_{CN} \cdot \beta_D \cdot C_N, \beta_L \cdot C_L\}.$$

For a particular environment of light, nutrients, organic matter and prey, an organism encounters different specific amounts of resources from the various encounter mechanisms (Figure 3). The smallest organisms get the highest encounter rate from diffusive encounter with dissolved organic matter. Diffusion feeding heterotrophic bacteria (osmo-heterotrophs) will therefore dominate among the smallest organisms. As size increases, encounter with photons becomes sufficiently high to make photosynthesis combined with diffusive uptake of inorganic nutrients optimal, i.e., the dominant strategy becomes phototrophy. The transition size is when carbon fixation by photosynthesis $\beta_L C_L = b_L l^2 C_L$ becomes equal to the diffusive encounter with dissolved organic matter $\beta_D C_{DOM} = b_D l C_{DOM}$, which occurs at a size:

$$l = \frac{C_{DOM} b_D}{C_L b_L} . \quad (4)$$

Cells larger than this size are expected to be light-limited phototrophs. When the cells reach a size

$$l = \frac{c_{CN}C_Nb_D}{C_Lb_L} \quad (5)$$

315

316 the diffusive uptake of inorganic nutrients becomes limiting (Mei *et al.* 2009).

317 Larger cells will still benefit from acquisition of carbon through the aid of

318 photosynthesis but they will be nutrient limited. At a size

319

$$l = \frac{c_{CN}C_Nb_D}{C_Fb_A} \quad (6)$$

320

321 active encounter with prey organisms provides the highest encounter rates, i.e.,

322 heterotrophic animals. There is a particular range where photosynthesis will

323 provide more carbon than active encounter (predation) but where active

324 encounter provides more nutrients than diffusive uptake of inorganic nutrients.

325 In this size-range a mixotrophic strategy is profitable, i.e. using photosynthesis,

326 either from ingested or own chloroplast, predominantly to provide carbon for

327 metabolism, and using active feeding to assimilate nutrients and carbon for

328 biomass synthesis (mixotrophs of type II and III; Stoecker, 1998).

329

330 The size range where a certain trophic strategy gives the highest yield depends

331 on the concentration of available resources. If, for example, the concentration of

332 prey organisms is increased, the lower size limit where active feeding gives the

333 highest yield is decreased. The transition size between the dominant feeding

334 strategies will therefore be different under oligotrophic conditions (high light

335 and low nutrient concentrations, such as summer surface conditions in seasonal

environments or oceanic regions) than under eutrophic conditions (low light and high nutrient concentrations, such as spring surface conditions in seasonal environments or conditions at depth) (Figure 4a+b). The general pattern of small diffusion feeders, medium phototrophs, and large active feeders is identical between oligotrophic and eutrophic environments, but the sizes where the transitions occur vary: oligotrophic conditions give rise to smaller phototrophs and a large size-range of mixotrophs, while eutrophic situations conditions lead to larger osmo-heterotrophic bacteria, phototrophs and mixotrophs. The general pattern fits well with the classical interpretation of the seasonal succession of cell size in temperate systems (Kjørboe, 1993): large (diatoms) cells dominate during nutrient rich spring conditions but are overtaken by smaller cells (dinoflagellates and cryptophytes), often with a mixotrophic strategy during the nutrient depleted summer conditions (Barton *et al.* 2013).

A compilation of the dominant trophic strategies according to size largely confirms the theoretical predictions while also highlighting the large overlap in the size-range between phototrophs, mixotrophs and small heterotrophs (Figure 4c). The overlap reflects that the compilation is based on the observations from various environmental conditions that, as demonstrated above, create a significant variation in the transition sizes where one trophic strategy gives a higher yield than another strategy.

Mobility

Movement is powered by muscles or flagellae and constrained by friction from the water. From an organism's perspective the nature of the water changes

dramatically with size: large organisms use their inertia to coast through the water while smaller organisms experience water as thick and sticky. Very small organisms have to cope with the random forces of molecules that induce Brownian motion (Dusenbery 2009). The hydromechanics of movement can therefore be divided into three regimes: an inertial regime, a viscous regime and a Brownian regime. Here we are mainly concerned with the difference between the inertial and viscous regimes. The hydrodynamic regime determines the forces upon the body, which in turn influences the optimal shape. In the viscous regime the dominating force is surface friction, which scales with the linear dimensions of the body. In the viscous regime it is therefore optimal to reduce the surface area, i.e. to be spherical (actually, the optimal shape is deviating slightly from spherical; Dusenbery, 2009). In the inertial regime the drag force is proportional to the projected frontal area of the organisms making it optimal to reduce this area by streamlining..

Whether an organism is in the inertial or viscous regime depends on the Reynolds number $Re = ul/\nu$ that describes the ratio between inertial and viscous forces operating on a body of size l moving at velocity u through water with kinematic viscosity $\nu \approx 10^{-2} \text{ cm}^2/\text{s}$. The crossover between the two regimes is at $Re \approx 20 - 30$ (Webb 1988). The scaling of swimming velocity with size in the two regimes differs: in the viscous regime the velocity was found empirically to scale as $l^{0.79}$ (Kiørboe, 2011) while in the inertial regime theoretic arguments predict a length scaling with exponents 0.42 (Ware 1978) or 0.5 (Bejan & Marden 2006); observation suggest a scaling $u \propto l^{0.45}$ (Figure 5a). The

empirical data indicate a crossover size between the viscous and inertial regime at body length of around 7 cm corresponding to a Reynolds number on the order of 1000. The relevance of size for body shape is evident (Figure 5b): small organisms do not appear constrained on their body shape, while fish and mammals are streamlined with an average aspect ratio around 0.25. Copepods are in between; they have a significantly larger aspect ratio than fish. During jumps, however, the Reynolds number becomes large thus giving them the advantage of a relatively slender body plan (Kjørboe et al. 2010).

Size and sensing

Actively feeding organisms perceive their prey by chemical or hydromechanical cues, vision, or echolocation. The range of sensing is determined by the size of the predator and the prey; a blue whale with an eye diameter of 15 cm sees much further than a fish larva with an eye diameter of 1 mm. The sense with the furthest range for organisms of a given size can be expected to dominate among organisms of that size. Organisms using more than one sense complicate the analysis of senses. For example, sharks use smell to follow the trail of a prey at great distances. When closing in on the prey, vision becomes important (Hueter et al. 2004). At distances below one meter they use electro-sensing for the precise localization of their prey (Collin & Whitehead 2004). Copepods are generally considered mechanosensing organisms, yet they can sense and follow the chemical trail of a settling marine snow particle (Kjørboe 2001) or the pheromone trail of a potential mate (Bagøien & Kjørboe 2005). Leaving such complications aside we nevertheless proceed to review estimates of the sensory

range of four senses where the sensing range depend on the size of the predator:
chemical sensing, sensing of hydromechanical signals, vision and echolocation.

Chemosensing

In that all organisms depend on chemistry in one way or another, it may be safely assumed that they have machinery for chemical sensing. The question is how chemosensing together with behavior can bring organisms into contact with remote resources. The way organism's experience the coherence of chemical gradients and trails is determined by individual size in relation to turbulent eddies. Turbulence is characterized by three length scales (Tennekes & Lumley 1972): the Batchelor scale, $\approx 10 \mu\text{m}$ in the upper ocean, where turbulence starts to erode the regularity of a gradient, the Kolmogorov scale $\approx 1000 \mu\text{m}$ where turbulence starts to impede the organism's ability to maintain direction, and the integral scale $\approx 1\text{-}10 \text{ m}$ where turbulent energy is injected by large-scale motions.

We distinguish between two modes of chemosensing: gradient climbing (e.g. bacterial run-tumble) and trail following (e.g. a shark following a prey trail). Gradient climbing relies on a chemical gradient set up by molecular diffusion of a solute from a source. The regularity of such gradients would be scale independent if it were not for turbulence. We can place an upper boundary for gradient climbing at between the Batchelor scale and the Kolmogorov scale, in the range from $10\text{-}1000 \mu\text{m}$. Another limitation of the ability to follow gradients created by molecular diffusion is whether the trail is diffusing faster than the

movement of the prey. This criterion sets an upper limit for predator size of 50 μm (Kiørboe 2011). For trail following, additional criteria come into effect: the movement of the target organism, the rate at which it releases solute and how well the searching organism can detect this solute above background levels. In any case, organisms smaller than the energy containing turbulent eddies will experience the trail as patchy and therefore need to search large areas relative to their own size to follow the trail. This scenario is relevant for organisms of a size between the Kolmogorov and the integral length scales, i.e. organisms smaller than 1 m. Organisms larger than the integral scale are able to integrate over the subscale trail details and follow a trail without detours. Trail following is therefore most advantageous for large organisms and/or quiescent environments, e.g. the deep oceans (Martens et al.).

Mechanosensing

Ambush feeders may sense their prey via the fluid mechanical disturbance created by a moving prey (reviewed by Kiørboe 2011). To enhance the sensory range they employ special sensory arrangements protruding from the body, like the long setae-studded antennules on copepods or the sensory hairs arranged along the slender body of chaetognaths (arrow worms). The fluid mechanical disturbance of a self propelling prey can be modelled as a stress-let which implies that the signal attenuates as the cube of the distance away from the prey (Visser 2001). The range that this signal can be sensed is

$R \approx (3 l_{\text{prey}}^2 l_{\text{sensor}} u_{\text{prey}} / u^*)^{1/3}$ where u^* is the detection limit of the velocity disturbance and l_{sensor} is the length of the sensor, approximately the size of the

predator. Using $u_{\text{prey}} = bl_{\text{prey}}^{0.74}$ and a predator-prey length ratio $B \approx 10$ the sensing distance is $R \approx cl^{1.24}$ with $c \approx 1.4 \text{ cm}^{-0.24}$ for $u^* = 33 \text{ } \mu\text{m/s}$ (Kjørboe 2011) (Figure 6). An upper range comes into effect when the turbulent shear γ across the body of the predator organism approaches the sensitivity; i.e. when $u^* = \gamma l$. For moderate turbulent shears found in the upper ocean (0.03 s^{-1} which in the middle of the typical range of 10^{-4} - 10^{-1} s^{-1} ; Visser & Jackson 2004), this happens for l in the range 500-1000 μm . Mechanosensing is therefore most advantageous for small organisms ($<1 \text{ cm}$) or on short ranges for large organisms.

Vision

Eyes contain photoreceptors that detect light and convert it into neuronal signals. The simple eyes of some microorganisms are only able to detect changes in the ambient light sufficient for detection of diurnal rhythms, orientation towards the surface and nearby movement. Active visual predation requires an eye with sufficient resolution to form an image and preferably also active optical machinery to focus a targeted object. With regards to feeding, the most important property of the eye is the distance at which it can discern a suitable prey.

[Sidebar 1 near here]

Dunbrack and Ware (1987) modelled the optical and sensing abilities of a camera eye to estimate the visual range of a predator of length l searching for

prey with a fixed fraction of the predator size (Sidebar 1). Two important conclusions emerge from their arguments: First, the sensing range scales as $l^{1.75}$ in clear water under high light conditions. Second the maximum range of large organism is limited by the optical properties of the water. Under perfect conditions the range is between 40-70 m (Davies-Colley & Smith 1995). The range decreases with the ambient light such that at depth, where the inherent contrast is low, visual range is mainly limited by the optical properties of the water.

A lower size limit of a functioning eye is determined by the finite size of the photoreceptor. Photoreceptors' functioning relies on opsin molecules (rhodopsin) stacked in rod cells with a width $d_{\text{rod}} \approx 1 \mu\text{m}$ (Curcio et al. 1990). Taking account of the universality of the opsin design for photoreception, we may consider this length a limiting factor for building eyes. Considering a minimal resolution of, say 100^2 for sufficient image formation, results in a retina size of $d_r \approx 0.1 \text{ mm}$. This is about 1/10 of the size of the smallest aquatic organisms with camera eyes: larval fish and cephalopods. Therefore, vision is only a viable sensing mode for organisms in the size range from a few millimetres and up.

Echolocation

Echolocation is an active sensing mode, where the animal emits ultrasonic calls and interprets the environment based upon the echo of these calls. It is common

for toothed whales (Odontocetes) and while it is also used for orientation, here we focus on echolocation and its role in prey detection.

We can estimate how the range R of echolocation scales with the size of the animal based on three assumptions: 1) The sensitivity of the ear P_0 is independent of the size of the animal, 2) the emitted power scales with an exponent p as $P_e \propto w^p \propto l^{3p}$, 3) we ignore frequency dependent attenuation of sound in seawater because this attenuation is small compared to the conical spread of the sound wave. In free space the emitted signal spreads as a conic beam resulting in the attenuation of the signal power as R^{-2} . The power of the reflected signal is $P_r \propto P_e l_{\text{prey}}^2 (2R)^{-2}$ where l_{prey}^2 is the area of the reflecting target and the factor 2 is because the signal attenuates both as it travels towards the target as well as when it returns. Inserting the power of the emitted signal and absorbing the factor 2 in the proportionality constant gives $P_r \propto l^{3p} l_{\text{prey}}^2 R^{-2}$. The distance where the strength of the returned signal is just at the sensitivity of the ear, i.e. $P_0 = P_r$, scales as $R \propto P_0^{-1/2} l_{\text{prey}} l^{3p/2}$. If the preferred prey size scales with the size of the predator, i.e. $l_{\text{prey}} \propto l$, then:

$$R \propto P_0^{-1/2} l^{1+3p/2}.$$

If the power of the emitted sound follows metabolic scaling, $p = 3/4$ then the exponent becomes $17/8$. This argument only provides the scaling of the sensing range; the factor can be found by fitting to data (Figure 6a).

525

526 *Size and sense*

527 The theoretic arguments outlined above identified three characteristic sizes
528 where one sense becomes more efficient than another: 1) an upper size limit for
529 gradient climbing at a predator size of around 100 μm ; 2) predators larger than
530 that 100 μm but smaller than 1 mm are expected to rely predominantly on
531 hydromechanical sensing, 3) a size where vision becomes viable for a predators
532 of around 1 cm, and 4) a size of around 1 meter or larger where predators are
533 able to realize the upper visible range of up to 80 meter in clear water. An
534 extension of the sensory range beyond this length can only be achieved by trail-
535 following chemical tracers or by echolocation.

536

537 Analysis of body size and senses used by marine organisms reveals that the
538 number of possible senses available to a predator increases with size (
539 Figure 6b). Large organisms typically combine several senses for foraging. The
540 lower size limit of vision around 1 cm is clearly borne out; this size indeed
541 corresponds to the smallest size of fish and cephalopods larvae. Some large life
542 forms do not use vision to detect prey, most notably the gelatinous zooplankton,
543 even though they are much larger than 1 cm. Seen in this perspective, the
544 strategy of gelatinous zooplankton is to avoid building a vertebrate body with its
545 associated high metabolic requirements to utilize the increasing sensing range
546 that vision provides but rather depend on an inflated body to increase the prey
547 encounter cross section (Kiørboe 2013). The superiority of vision declines with

548 ambient light so the relative disadvantage of gelatinous zooplankton versus fish
549 diminishes in turbid water or in deep waters (Sørnes & Aksnes 2004).

550 **Life history and progeny size**

551 Though obvious on the individual level, the concept of size becomes ambiguous
552 when applied at the species level since all life differs in the size of adults and
553 progeny; even unicellular organisms need to double their size before they can
554 divide. The difference between adult and progeny size is most extreme among
555 the teleosts (bony fish) where the weight ratio between adults and larvae can be
556 up to 10^8 for bluefin tuna.

557

558 [sidebar 2 near here]

559

560 *Optimal life history theory*

561 The evolution of life history with a pronounced difference between adult and
562 offspring size can be understood from optimal life history theory (Andersen et al.
563 2008, Christiansen & Fenchel 1979). If we assume 1) standard metabolic scaling
564 of consumption $= Aw^n$ with $n \approx 3/4$ (West et al. 1997); 2) metabolic scaling of
565 mortality $\propto Aw^{n-1}$ (Andersen & Beyer 2006, Hirst & Kiørboe 2002, Peterson &
566 Wroblewski 1984); and 3) determinate growth, then the lifetime reproductive
567 output R_0 becomes (Sidebar 2):

568

$$R_0 = \frac{\epsilon}{2\alpha} \left(\frac{W}{w_0} \right)^{1-\alpha}, \quad (7)$$

569

where W/w_0 is the ratio between the weight at maturation and weight of offspring, ϵ is the efficiency of reproduction and α is the physiological mortality, which is less than 1 (Andersen *et al.* 2008). Because the exponent $1 - \alpha$ is positive R_0 is an increasing function of W/w_0 . The metabolic assumptions thus predict an evolutionary pressure towards a life history with as large a ratio between adult size and offspring size as possible. Since no organisms has an infinite ratio between adult size and offspring size, a full understanding of what limits actual offspring size cannot be achieved from optimal life history theory based on metabolic scaling laws alone; the actual offspring size will be limited by other processes.

Offspring size strategies

Observed offspring size strategies employed by marine life can roughly be partitioned into two groups: a “fixed-ratio” strategy where offspring size is a constant fraction of the adult size and a “small-eggs” strategy where offspring size is the same, independent of adult size (Neuheimer *et al.*) (Figure 7). Crustaceans, cartilaginous fish and whales employ the fixed-ratio strategy with an adult:offspring weight ratio around 100:1. The metabolic optimal life history theory (eq. 7) is unable to predict the fixed-ratio strategy. For marine mammals the fixed-ratio strategy can be explained by the need to perform parental care (Shine 1978). For the other groups, the fixed-ratio strategy can be explained by an elaboration of the evolutionary argument in sidebar 2, to account for density dependent effects (Olsson *et al.*). Such elaboration shows that the strategy that maximizes W/w_0 is only optimal if the

offspring do not experience density dependent effects right at the time of hatching. If they do experience density dependent survival early in life, an evolutionary stable strategy with $W/w_0 \approx 100$ emerges.

Transitions between life forms

We have reviewed how size influences resource acquisition, mobility, ability to sense prey, and life-history strategy, based on theoretical arguments and cross-species empiric analyses. We now use these relations to understand the mechanisms behind the transitions between the seven realms of marine life: molecular life, osmo-heterotrophic bacteria, unicellular phototrophs, unicellular mixotrophs and heterotrophs, planktonic multi-cellular heterotrophs with ontogenetic growth, visually foraging poikilotherms, and homeothermic animals (Figure 1 and Table 1). These seven realms correspond to the traditional taxonomic division of life between viruses, bacteria, phytoplankton, uni- and multicellular zooplankton, fish and marine mammals. Our alternative naming reflects the function of the groups and highlights the factor that determines the characteristic size where there is a transition between the groups.

A central theme is that development of larger size opens new possibilities for resource acquisition and sensing. Examples are how the battery of available senses increases with size (Figure 6), how the emergence of multicellularity makes it possible to increase the adult:offspring size ratio and thereby increase fitness (Sidebar 2), or how mortality decreases with size. Larger size therefore increases the competitive

edge, provides access to new resources as well as increases survival. The sizes where new possibilities appear often mark a transition between the major life forms because the utilization of new senses etc. require fundamental changes in body plan and life strategy.

From viruses to cells

The smallest size of a cell is around 10^{-15} g_c with a diameter around 0.1 – 1 μm . Organisms this small are believed to be functionally limited by metabolic constraints (Kempes et al. 2012) and the size of non-scalable components: genome size (DeLong et al. 2010) and in particular the cell wall (Raven 1994). The wall size alone can be used to calculate a lower limit for cell size: The wall has a mass $c_{\text{wall}}d^2$ and the cell itself cd^3 where c_{wall} and c are constants. If we ignore the genome a theoretical lower limit to cell size is when all cell mass is used by the wall:

$$d_{\text{limit}} = \frac{c_{\text{wall}}}{c} \quad (8)$$

For a 0.5 μm cell the wall comprises about 30 % of the total mass (Raven 1994), so $c_{\text{wall}}/c \approx 0.3 \times 0.5 \mu\text{m}$. This gives a lower limit cell size of $d_{\text{limit}} \approx 0.15 \mu\text{m}$.

From osmo-heterotrophs to phototrophs

The smallest unicellular organisms are heterotrophic bacteria feeding on dissolved organic matter encountered through diffusion. At a diameter

$C_{\text{DOM}}b_D/(C_Lb_L)$ (eq. 4), it becomes favourable to fix inorganic carbon through photosynthesis instead of relying on dissolved organic matter. This size depends on the relative concentrations of dissolved organic matter C_{DOM} and light C_L , but it can be as small as 10^{-14} g_c in the upper photic zone with concentrations of dissolved organic matter $C_{\text{DOM}} \approx 5 \mu\text{g}_c/\text{l}$ and abundant light ($C_L \approx 7 \text{ J day}^{-1}\text{m}^{-2}$) and increases as a light decreases (Figure 4).

From phototrophs to heterotrophs

The smallest phototrophs are expected to be carbon limited (which in practice means that they are limited by the amount of light since dissolved inorganic carbon is assumed to be plentiful), while the largest phototrophs are expected to be nutrient limited. This difference emerges from the different scaling of nutrient encounter that scales with l^1 and light encounter that scales with l^2 (Eqs. 2 and 3 and Figure 3). As before, the exact sizes where the transitions between light limited phototrophs, nutrient limited phototrophs, and heterotrophs occur depend on the specific conditions of dissolved nutrients, light and suitable prey (Figure 4b). An order-of-magnitude estimation of the characteristic transition between phototrophs and pure heterotrophs is 10^{-7} g_c ($l \approx 6 \times 10^{-2}$ cm), but it can vary between 10^{-8} g_c in low light and high nutrients situations and 10^{-5} g_c in situations of high light.

The size that marks the transition between phototrophs and heterotrophs is blurred by a large group of mixotrophic organisms that acquire nutrients and carbon for biomass synthesis from phagotrophy while photosynthesis primarily provides carbon for metabolism. The mixotrophic strategy is most favourable for organisms with sizes in the transition between phototrophy and heterotrophy. The size range where the mixotrophic strategy is favourable varies with environmental conditions: it is vanishingly small in eutrophic conditions and increases to more than a factor 10 in diameter in oligotrophic conditions, in agreement with observations (Barton et al. 2013).

Unicellular to multicellular life

The drive to develop larger size eventually leads to multicellular organisms. Multicellularity opens the possibility of specialized tissue for, e.g., sensory organs. Among microscopic metazoans the dominant group of copepods has developed sensory apparatus to detect prey via hydromechanical cues and appendages to generate feeding currents and make jumps to escape predators. We have not developed a specific argument for the size where the transition to multicellularity occurs, but since life-history theory predicts that increasing offspring-adult size ratio increases lifetime reproductive output (Eq. 7), it is likely to occur at the smallest possible size. DeLong *et al.* (2010) argue that this is when it becomes possible to develop a fractal delivery network, around 10^{-6} g_c ($\approx 1 \mu\text{m}$). The drive towards minimization of offspring and maximization of adult size means that each metazoan group strives to extend its size range, but is

only able to do so within the limits defined by the sizes where there is a
breakdown in a scaling relationship describing a vital function.

From copepods to fish

Fish (including cephalopods) are the dominant organisms in the size-range from
1 mg_{ww} to about 100 kg (1 cm to 2 m). Fish are characterized by being
streamlined, visual predators. At a size smaller than 1 mg_{ww} the dominating
organisms are blind copepods, with a very non-streamlined body plan. The
transition size between these two very different life forms is characterized by the
transition from the superior sensing mode being mechanosensing to vision and
the transition from a viscous to an inertial hydromechanical regime. The change
in hydromechanical regime explains the slender fish shape, but it also entails a
change in feeding mode. Fish larvae employ suction feeding, which becomes
increasingly difficult the smaller they are (China & Holzman 2014). Probably the
most important transition is in sensing, with the lower size limit of fish
coinciding with the lower size of a functioning eye. Were fish to make smaller
eggs their larvae would be unable to compete with the tactile sensing copepod
with a morphology designed for optimal movement and prey capture in a viscous
fluid environment; were copepods to become larger they would be outcompeted
by visually sensing fish with streamlined bodies.

From fish to whales

Whales are the largest organisms in the oceans, occupying the size range from
about 100 kg and up. It is tempting to attribute the transition from fish to whales

to the appearance of echolocation as a possible sensing mode. However, only toothed whales employ echolocation for sensing, whereas baleen whales rely on the same senses as fish. If there are no change in the power law relationships determining sensing and food encounter, why, then, have teleosts not evolved even larger sizes than the few hundred kilos of the largest fish (bluefin tuna or sunfish with maximum weights of 450 and 1000 kg_{ww})? We propose two arguments for the transition between fish and marine mammals: a metabolically based upper limit of a water-breathing organism (Freedman & Noakes 2002; Makarieva et al. 2004, Supp.) and a lower size limit of a homeothermic (warm-blooded) organism.

We have focused on acquisition of resources in terms of carbon and nutrients, but heterotrophs also need oxygen to fuel their metabolism. The absorption of oxygen through gills is limited by the surface of the gills. Since the surface of gills is fractal it will scale with an exponent between $2/3$ and 1, probably very close to the metabolic exponent of $3/4$. The acquisition of oxygen therefore scales with a similar exponent as metabolism, so the relative ability to acquire food and oxygen is independent of size. However, larger organisms accumulate heat created by activity and use this to elevate their metabolism. Notable examples are the scombroids (tuna and marlin) and pelagic sharks (Block 1991). A high body temperature means higher activity and therefore higher predatory success against slower heterothermic (cold-blooded) prey. Such an increase in metabolism will eventually require more oxygen than can be obtained by pumping water over the gills. This problem is solved by ram ventilation, which

provides a higher flow of water around the gills and therefore a higher oxygen absorption rate. Evidence for this is provided by the largest fish being either very active ram-ventilating (large scombroids or sharks) or relatively sluggish pumping (sunfish). We conjecture that it would be impossible for fish to develop homeothermy as a means of competing with marine mammals; the solubility of oxygen in water is simply too low to fuel a homeothermic metabolism. Marine mammals fuel their high homeothermic metabolism by breathing air, which has a much higher solubility of oxygen than water.

For homeotherms the loss of body heat should be included in the energy budget as this defines a lower limit for the size of a homeotherm (Haldane 1928). Heat loss is a surface process that scales as $\propto \kappa w^{2/3}$ where κ is the thermal conductivity of water. Since organisms wish to minimize heat loss their surface is not fractal and the exponent is not larger than $2/3$. The energy for heating comes from the acquisition of resources (oxygen and food), which scales metabolically as $Aw^{3/4}$. The size where there is a balance between loss of heat and acquisition of resources defines a lower limit of homeothermy as $(A/\kappa)^{12}$ (Andersen et al. 2008). This lower limit is very sensitive to the value of the parameters A and κ since their ratio is raised to a high exponent. For example, the ratio between the lower limits calculated for a marine and a terrestrial habitat is the ratio between the heat conductivity in air and water (≈ 20), raised to power 12 which gives 4×10^{15} . This factor is much larger than the ratio between the smallest whale, a harbour porpoise calf of around 10 kg, and the smallest terrestrial homeotherm, an Etruscan shrew (*Suncus etruscus*) at around 0.1 g. Nevertheless it seems

evident that the smallest land animals are limited by loss of heat, e.g. shrews huddle together to conserve heat, so how can whales manage to attain a small size in the face of a larger heat loss? We hypothesise that whales do that by having an insulating layer of blubber. To achieve a lower size of 10 kg (a factor 10^6 smaller than predicted), whales need to decrease heat losses by a factor $10^{6/12} \approx 3.2$ relative to terrestrial animals, which is not out of scope.

Beyond size

We posit that individual size is the most important trait characterizing a pelagic organism. Knowing the size, it is possible to estimate, often within an order of magnitude, the metabolic rate, the clearance rate, the swimming speed and the sensory range. We have shown how that information facilitates inference of trophic strategy, sensory mode, body shape, and, to some degree, reproductive strategy. Though important, we have largely ignored the subtle interplay between temperature, oxygen concentration and size (Verberk & Atkinson 2013). Even though size can be characterized as a “master trait” (Litchman & Klausmeier 2008), it is not the only trait that characterizes an organism. The relevant question is then which other traits best characterize the variation around the mean in the reviewed relations with size (Figure 2, 5 and 7). We propose three candidate traits to consider: predator-prey size ratio, “feeding mode” for heterotrophic metazoans and “jellyness”.

Among heterotrophic metazoans there appear to be two dominant strategies to predator-prey size ratio: a fixed predator-prey length ratio in the range 10-100, which is the strategy followed by most fish and copepods (Barnes et al. 2008), or

a strategy aimed at preying on organisms much smaller than the predator. The small-prey strategy is used by the largest zooplankton, the pelagic tunicates, and by the largest vertebrates, the whale sharks and the baleen whales. Organisms with a large predator-prey size ratio rely on filtering the water to catch the prey. It is presently unknown what drives the development of the two alternative, but apparently equally competitive, strategies.

The feeding mode determines whether an actively feeding predator encounters its prey through ambushing or cruising. It is often assumed that predation pressure is a function of size only and therefore independent of feeding strategy or sensing mode. This is not quite true. It is becoming increasingly evident that feeding strategy is associated with a trade-off in mortality: an ambush feeder will encounter less prey than a cruising predator but it will also have less exposure to predation and therefore lower mortality. A quantitative demonstration of this trade-off has been made for zooplankton based on laboratory experiments (Kjørboe 2013b) and the importance for the seasonal succession has been modelled (Mariani et al. 2013). These trade-offs likely apply at least qualitatively to other predators, e.g. fish.

A related trade-off is the development of a gelatinous body (jellyfish, box jellies and pelagic tunicates). We argued in section “sensing” that visual predators would be superior to predators sensing their prey through hydromechanical forces. However, the inflated body size of gelatinous organisms results in a large encounter cross-section and hence a higher clearance rate than a non-gelatinous

organisms with the same carbon body mass. This is what makes the jelly-strategy effective even in the same size range where visual predation is possible (Acuña *et al.* 2011), particularly under low light conditions (Sørnes & Aksnes 2004). At the same time the gelatinous body makes the organism less attractive to predators thereby lowering its mortality. These two examples show how the general "rules" inferred from size scaling of encounter, mobility, and sensing can be transgressed by other traits.

Acknowledgements

KHA thanks Mick Follows for hospitality at MIT while the draft of this manuscript was written. This work is part of the "Centre for Ocean Life", a VKR center of excellence supported by the Villum foundation

Literature cited

- Acuña JL, López-Urutia Á, Colin S. 2011. Faking giants: the evolution of high prey clearance rates in jellyfishes. *Science*. 333(6049):1627–29
- Aksnes D, Egge J. 1991. A theoretical model for nutrient uptake in phytoplankton. *Mar. Ecol. Prog. Ser.* 70(1980):65–72
- Aksnes D, Utne A. 1997. A revised model of visual range in fish. *Sarsia*, pp. 137–47
- Andersen KH, Beyer JE. 2006. Asymptotic size determines species abundance in the marine size spectrum. *Am. Nat.* 168:54–61
- Andersen KH, Beyer JE, Pedersen M, Andersen NG, Gislason H. 2008. Life-history constraints on the success of the many small eggs reproductive strategy. *Theor. Popul. Biol.* 73(4):490–97

- 828 Ara R, Amin SMN, Mazlan AG, Arshad A. 2013. Morphometric variation among six families of
829 larval fishes in the Seagrass-Mangrove ecosysetm of Gelang Patah, Johor, Malaysia. *Asian J.*
830 *Anim. Vet. Adv.* 8(2):247–56
- 831 Bagøien E, Kiørboe T. 2005. Blind dating – mate finding in planktonic copepods. I. Tracking the
832 pheromone trail of *Centropages typicus*. *Mar. Ecol. Prog. Ser.* 300:105–15
- 833 Barnes C, Bethea DM, Brodeur RD, Spitz J, Ridoux V, et al. 2008. Predator and prey body sizes in
834 marine food webs. *Ecology.* 89(3):881
- 835 Barton AD, Finkel Z V., Ward B a., Johns DG, Follows MJ. 2013. On the roles of cell size and trophic
836 strategy in North Atlantic diatom and dinoflagellate communities. *Limnol. Oceanogr.*
837 58(1):254–66
- 838 Bejan A, Marden JH. 2006. Unifying constructal theory for scale effects in running, swimming and
839 flying. *J. Exp. Biol.* 209(Pt 2):238–48
- 840 Berg HC, Purcell EM. 1977. Physics of chemoreception. *Biophys. J.* 20:193–219
- 841 Block BA. 1991. Evolutionary novelties: how fish have built a heater out of muscle. *Am. Zool.*
842 31:726–42
- 843 Boudreau PR, Dickie LM. 1992. Biomass spectra of aquatic ecosystems in relation to fisheries
844 yield. *Can. J. Fish. Aquat. Sci.* 49(8):1528–38
- 845 Charnov EL. 1993. *Life History Invariants*. Oxford University Press, Oxford, England
- 846 China V, Holzman R. 2014. Hydrodynamic starvation in first-feeding larval fishes. *Proc. Natl. Acad.*
847 *Sci. U. S. A.* 111(22):8083–88
- 848 Christiansen FB, Fenchel TM. 1979. Evolution of marine invertebrate reproductive patterns.
849 *Theor. Popul. Biol.* 16:267–82

- 850 Cohen J, Pimm S, Yodzis P, Saldaña J. 1993. Body sizes of animal predators and animal prey in
851 food webs. *J. Anim. Ecol.* 62:67–78
- 852 Collin SP, Whitehead D. 2004. The functional roles of passive electroreception in non-electric
853 fishes. *Anim. Biol.* 54:1–25
- 854 Curcio CA, Sloan KR, Kalina RE, Hendrickson AE. 1990. Human photoreceptor topography. *J.*
855 *Comp. Neurol.* 292(4):497–523
- 856 Davies-Colley RJ, Smith DG. 1995. Optically pure waters in Waikoropupu ('Pupu') Springs,
857 Nelson, New Zealand. *New Zeal. J. Mar. Freshw. Res.* 29:251–56
- 858 DeLong JP, Okie JG, Moses ME, Sibly RM, Brown JH. 2010. Shifts in metabolic scaling, production,
859 and efficiency across major evolutionary transitions of life. *Proc. Natl. Acad. Sci. U. S. A.*
860 107(29):12941–45
- 861 Dunbrack RL, Ware DM. 1987. Energy constraints and reproductive trade-offs determining body
862 size in fishes. In *Evolutionary Physiological Ecology*, ed. P Calow, pp. 191–218
- 863 Dusenbery DB. 2009. *Living at Micro Scale: The Unexpected Physics of Being Small*. Harvard
864 University Press
- 865 Edwards KF, Thomas MK, Klausmeier CA, Litchman E. 2012. Allometric scaling and taxonomic
866 variation in nutrient utilization traits and maximum growth rate of phytoplankton. *Limnol.*
867 *Oceanogr.* 57(2):554–66
- 868 Fenchel T. 1974. Intrinsic rate of natural increase: the relationship with body size. *Oecologia.*
869 14:317–26
- 870 Fenchel T. 1984. Suspended Marine Bacteria as a Food Source. *Flows Energy Mater. Mar. Ecosyst.*
871 *NATO Conf. Ser.* 11:301–15

- 872 Fenchel T, Finlay BJ. 2004. The ubiquity of small species: patterns of local and global diversity.
873 *Bioscience*. 54(8):777–84
- 874 Fiksen Ø, Follows M, Aksnes D. 2013. Trait-based models of nutrient uptake in microbes extend
875 the Michaelis-Menten framework. *Limnol. Ocean.* 58(1):193–202
- 876 Finkel ZV. 2001. Light absorption and size scaling of light-limited metabolism in marine diatoms.
877 *Limnol. Oceanogr.* 46(1):86–94
- 878 Freedman JA, Noakes DLG. 2002. Why are there no really big bony fish? A point-of-view on
879 maximum body size in teleosts and elasmobranchs. *Rev. Fish Biol. Fish.* 12:403–16
- 880 Froese R, Pauly D. 2013. *FishBase*. www.fishbase.org
- 881 Gillooly J, Charnov E, West G, Savage V, Brown J. 2002. Effects of size and temperature on
882 developmental time. *Nature*. 417:70–73
- 883 Haldane JBS. 1928. On being the right size. In *A Treasure of Science*, p. 321
- 884 Hansen B, Bjørnsen PK, Hansen PJ. 1994. The size ratio between planktonic predators and their
885 prey. *Limnol. Oceanogr.* 39(2):395–403
- 886 Hansen PJ, Bjørnsen PK, Hansen BW. 1997. Zooplankton grazing and growth: scaling within the
887 2--2,000 μm body size range. *Limnol. Oceanogr.* 42(4):687–704
- 888 Hemmingsen AM. 1960. Energy metabolism as related to body size and respiratory surfaces, and
889 its evolution. *Rep. Steno Mem. Hosp.* 9(11):7–110
- 890 Hirst AG, Kiørboe T. 2002. Mortality of marine planktonic copepods: global rates and patterns.
891 *Mar. Ecol. Prog. Ser.* 230:195–209
- 892 Holling CS. 1959. Some characteristics of simple types of predation and parasitism. *Can. Entomol.*
893 91:385–98

- 894 Hueter RE, Mann DA, Maruska KP, Sisneros JA, Demski LS. 2004. Sensory biology of
895 elasmobranchs. *Biol. sharks their Relat.*, pp. 325–68
- 896 Huntley ME, Zhou M. 2004. Influence of animals on turbulence in the sea. *Mar. Ecol. Prog. Ser.*
897 273:65–79
- 898 Kempes CP, Dutkiewicz S, Follows MJ. 2012. Growth, metabolic partitioning, and the size of
899 microorganisms. *Proc. Natl. Acad. Sci. U. S. A.* 109(2):495–500
- 900 Kiørboe T. 1993. Turbulence, phytoplankton cell size, and the structure of pelagic food webs. *Adv.*
901 *Mar. Biol.* 29:1–72
- 902 Kiørboe T. 2001. Formation and fate of marine snow: small-scale processes with large-scale
903 implications. *Sci. Mar.* 65(Supp. 2):57–71
- 904 Kiørboe T. 2011. How zooplankton feed: mechanisms, traits and trade-offs. *Biol. Rev. Camb.*
905 *Philos. Soc.* 86(2):311–39
- 906 Kiørboe T. 2013. Zooplankton body composition. *Limnol. Oceanogr.* 58:1843–50
- 907 Kiørboe T, Andersen A, Langlois VJ, Jakobsen HH. 2010. Unsteady motion: escape jumps in
908 planktonic copepods, their kinematics and energetics. *J. R. Soc. Interface.* 7(52):1591–1602
- 909 Kiørboe T, Hirst AC. 2014. Shifts in mass-scaling of respiration, feeding, and growth rates across
910 life-form transitions in marine pelagic organisms. *Am. Nat.* 183(4):E118–30
- 911 Klausmeier C, Litchman E, Daufresne T, Levin S. 2004. Optimal nitrogen-to-phosphorus
912 stoichiometry of phytoplankton. *Nature.* 429:171–74
- 913 Kleiber M. 1932. Body size and metabolism. *Hilgardia.* 6:315–53
- 914 Litchman E, Klausmeier CA. 2008. Trait-Based Community Ecology of Phytoplankton. *Annu. Rev.*
915 *Ecol. Evol. Syst.* 39(1):615–39

- 916 Litchman E, Klausmeier CA, Schofield OM, Falkowski PG. 2007. The role of functional traits and
917 trade-offs in structuring phytoplankton communities: scaling from cellular to ecosystem
918 level. *Ecol. Lett.* 10(12):1170–81
- 919 Makarieva AM, Gorshkov VG, Bai-Lian L. 2004. Ontogenetic growth: models and theory. *Ecol.*
920 *Modell.* 176:15–26
- 921 Marañón E, Cermeño P, López-Sandoval DC, Rodríguez-Ramos T, Sobrino C, et al. 2013. Unimodal
922 size scaling of phytoplankton growth and the size dependence of nutrient uptake and use.
923 *Ecol. Lett.* 16(3):371–79
- 924 Mariani P, Andersen KH, Visser AW, Barton AD, Kiørboe T. 2013. Control of plankton seasonal
925 succession by adaptive grazing. *Limnol. Oceanogr.* 58(1):173–84
- 926 Martens EA, Wadhwa N, Jacobsen NS, Lindeman C, Andersen KH, Visser AW. Size Structures
927 Sensory Hierarchy in Ocean Life. *Submitt. Publ.*
- 928 May R, Godfrey J. 1994. Biological diversity: differences between land and sea. *Proc. R. Soc. B Biol.*
929 *Sci.* 343:105–11
- 930 May RM. 1975. Patterns of species abundance and diversity. *Ecol. Evol. communities*, pp. 81–120
- 931 Mei Z-P, Finkel Z V, Irwin AJ. 2009. Light and nutrient availability affect the size-scaling of growth
932 in phytoplankton. *J. Theor. Biol.* 259(3):582–88
- 933 Morel A, Bricaud A. 1981. Theoretical results concerning light absorption in a discrete medium,
934 and application to specific absorption of phytoplankton. *Deep Sea Res. Part.* 28A(11):1375–
935 1981
- 936 Morioka S, Vongvichith B, Phommachan P, Chantasone P. 2013. Growth and morphological
937 development of laboratory-reared larval and juvenile bighead catfish *Clarias*
938 *macrocephalus* (Siluriformes: Clariidae). *Ichthyology Res.* 60:16–25

- 939 Moser HG, Sumida BY, Ambrose DA, Sandknop EM, Stevens EG. 1986. Development and
 940 distribution of larvae and pelagic juveniles of ocean whitefish, *Caulolatilus princeps*, in the
 941 Calcofi survey region. *CalCOFI Rep.* XXVII:
- 942 Munk WH, Riley GA. 1952. Absorption of nutrients by aquatic plants. *J. mar. Res.* 11:215–40
- 943 Neuheimer AB, Hartvig M, Heuschele J, Hylander S, Kiørboe T, et al. Adult and offspring size in the
 944 ocean over 17 orders of magnitude follows two life-history strategies. *Submitt. Publ.*
- 945 Northmore D, Volkmann FC, Yager D. 1978. Vision in fishes: colour and pattern. In *The Behavior*
 946 *of Fish and Other Aquatic Animals*, ed. DI Mostofsky, pp. 79–136. Academic press
- 947 Oka S, Higashiji T. 2012. Early Ontogeny of the big roughy *Gephyroberex japonicus*
 948 (Beryciformes: Trachichthyidae) in captivity. *Ichthyology Res.* 59:282–85
- 949 Olsson K, Gislason H, Andersen KH. Dual offspring size strategies in fish. *Submitt. Publ.*
- 950 Peters RH. 1983. *The Ecological Implications of Body Size*. Cambridge University Press
- 951 Peterson I, Wroblewski J. 1984. Mortality Rate of Fishes in the Pelagic Ecosystem. *Can. J. Fish.*
 952 *Aquat. Sci.* 41:1117–20
- 953 Rall BC, Brose U, Hartvig M, Kalinkat G, Schwarzmüller F, et al. 2012. Universal temperature and
 954 body-mass scaling of feeding rates. *Philos. Trans. R. Soc. B Biol. Sci.* 367:2923–34
- 955 Raven JA. 1994. Why Are There No Picoplanktonic O₂ Evolvers with Volumes Less Than 10⁻¹⁹
 956 m³? *J. Plankton Res.* 16:565–80
- 957 Reuman DC, Gislason H, Barnes C, Mélin F, Jennings S. 2014. The marine diversity spectrum. *J.*
 958 *Anim. Ecol.* 83(4):963–79
- 959 Sambilay VC. 1990. Interrelationships between swimming speed, caudal fin aspect ratio and body
 960 length of fishes. *Fishbyte.* 8(3):16–20

- 961 Schwaderer AS, Yoshiyama K, de Tezanos Pinto P, Swenson NG, Klausmeier CA, Litchman E. 2011.
 962 Eco-evolutionary differences in light utilization traits and distributions of freshwater
 963 phytoplankton. *Limnol. Oceanogr.* 56(2):589–98
- 964 Sheldon R, Prakash A. 1972. The size distribution of particles in the ocean. *Limnol. Oceanogr.*
 965 XVII(May):327–40
- 966 Sheldon RW, Sutcliffe Jr. WH, Paranjape MA. 1977. Structure of pelagic food chain and
 967 relationship between plankton and fish production. *J. Fish. Res. Board Canada.* 34:2344–53
- 968 Shine R. 1978. Propagule size and parental care: the “safe harbor” hypothesis. *J. Theor. Biol.*
 969 75(4):417–24
- 970 Sørnes TA, Aksnes DL. 2004. Predation efficiency in visual and tactile zooplanktivores. *Limnol.*
 971 *Oceanogr.* 49(1):69–75
- 972 Stoecker DK. 1998. Conceptual models of mixotrophy in planktonic protists and some ecological
 973 and evolutionary implications. *Eur. J. Protistol.* 34:281–90
- 974 Taguchi S. 1976. Relationship between photosynthesis and cell size of marine diatoms. *J. Phycol.*
 975 12:185–89
- 976 Tambi H, Flaten G, Egge J, Bødtker G, Jacobsen A, Thingstad TF. 2009. Relationship between
 977 phosphate affinities and cell size and shape in various bacteria and phytoplankton. *Aquat.*
 978 *Microb. Ecol.* 57:311–20
- 979 Tennekes H, Lumley JL. 1972. *A First Course in Turbulence.* The MIT press
- 980 Throndsen J, Hasle G, Tangen K. 2003. *Norsk Kystplanktonflora.* Almater Forlag
- 981 Tomas CR. 1997. *Identifying Marine Phytoplankton.* Academic press

- 982 Verberk WCEP, Atkinson D. 2013. Why polar gigantism and Palaeozoic gigantism are not
983 equivalent: effects of oxygen and temperature on the body size of ectotherms. *Funct. Ecol.*
984 27(6):1275–85
- 985 Visser A. 2001. Hydromechanical signals in the plankton. *Mar. Ecol. Prog. Ser.* 222:1–24
- 986 Visser AW, Jackson GA. 2004. Characteristics of the chemical plume behind a sinking particle in a
987 turbulent water column. *Mar. Ecol. Prog. Ser.* 283:55–71
- 988 Ware DM. 1978. Bioenergetics of pelagic fish: theoretical change in swimming speed and ration
989 with body size. *J. Fish. Res. Board Canada.* 35:220–28
- 990 Watkins JL, Brierley AS. 2002. Verification of the acoustic techniques used to identify Antarctic
991 krill. *ICES J. Mar. Sci.* 59(6):1326–36
- 992 Webb P. 1988. Simple physical principles and vertebrate aquatic locomotion. *Am. Zool.*
993 28(2):709–25
- 994 West GB, Brown JH, Enquist BJ. 1997. A general model for the origin of allometric scaling laws in
995 biology. *Science.* 276(5309):122–26
- 996 Winberg GG. 1956. Rate of metabolism and food requirements of fishes. *J. Fish. Res. Board Canada.*
997 194:1–253
- 998

999

1000 **Acronyms and definitions**

1001

1002 **Power law:** $y = ax^b$ with factor a and exponent b . Linear regression employs a
1003 logarithmic transformation: $\log y = \log a + bx$, with $\log a$ being “intercept” and b
1004 the “slope”.

1005

1006 **Poikilotherm:** An organism that maintains the same body temperature as the
1007 environment, in contrast to a **homeotherm** which maintains a constant body
1008 temperature due to internal heat sources.

1009

1010 **Protists** are simple, typically unicellular, eukaryotic organisms, living in aquatic
1011 environments.

1012

1013 An organisms’ **trophic strategy** describes how it gathers nourishment. The
1014 suffix “troph” derives from ancient greek: *trophe*=food, nourishment; *drepo*=to
1015 gather.

1016

1017 **Phototrophs** rely on photosynthesis as their carbon source and use
1018 **osmotrophic** diffusive uptake of nutrients. In contrast **phagotrophs** up carbon
1019 and nutrients by absorbing other living organisms. **Mixotrophs** employ a mixed
1020 strategy, typically combining photosynthesis with phagotrophy.

1021 *Note for production: The above definition is longer than 20 words (37), but it also*
1022 *defines four terms.*

1023 **Cartilaginous fish** (*Chondrichthyes*) are fish with skeletons made of cartilage
1024 rather than bone, containing elasmobranchs (sharks, rays and skates) and
1025 Holocephalii (“ghost sharks”).
1026
1027 **Cephalopods** are squid, octopi and cuttlefish, commonly referred to as “inkfish”.
1028
1029 The **physiological mortality** is the ratio between mortality and weight-specific
1030 consumption. With metabolic scaling of uptake $Aw^{3/4}$ and mortality $cw^{-1/4}$ the
1031 physiological mortality becomes $\alpha = c/A$.
1032
1033 **Stresslet**: A stokes flow produced by 2 co-linear anti-parallel point forces acting
1034 on a fluid.

1035

1036 Table 1. Characteristic sizes of transitions between major realms of life in the
 1037 ocean.

Transition	Size	Notes
Lower size of a cell	$0.15 \mu\text{m} \approx 10^{-15} \text{ g}_\text{C}$	Limited by cell wall and to a lesser extent genome size (Eq. 8)
Osmo-heterotrophs to phototrophs	10^{-14} to $10^{-13} \text{ g}_\text{C}$	Transition from diffusion feeding on DOM to photosynthesis (Eq. 4).
Phototrophs to mixotrophs	$10^{-8} \text{ g}_\text{C}$	Transition from acquiring inorganic nutrients by diffusion feeding to acquiring nutrients by active feeding (Eq. 5)
Mixotrophs to heterotrophs	$10^{-7} \text{ g}_\text{C}$ (10^{-8} to $10^{-5} \text{ g}_\text{C}$)	Acquisitions of carbon and nutrients solely by predation through active feeding (Eq. 6)
Single- to multicellular organisms	$10^{-6} \text{ g}_\text{C}$	Development of vascular networks.
Copepods to fish	$\approx 1 \text{ mg}_{\text{ww}}$	Smallest size of a functional camera eye
Fish to whales	$\approx 10 \text{ kg}_{\text{ww}}$	Lower size of maintaining a homeothermic metabolism

1038

1039

Sidebar 1: The Dunbrack and Ware model of visual range

The maximum visual range in clear water can be estimated by considering the properties of a pin-hole camera eye as done in a largely unrecognized work by Dunbrack and Ware (1987). Here we provide a simplified derivation of their argument, which corrects a number of minor errors.

The projection of a visual image of a prey on the retina of a predator activates a number of visual elements n proportional to the area of the projected image multiplied by the density of visual elements. Since we are interested in the maximum distance R that an object can be discerned we can assume that the distance is large relative to the diameter of the eye such that the curvature of the eye can be ignored. The number of activated visual elements is: $n \propto \rho l_{\text{eye}}^2 l_{\text{prey}}^2 R^{-2}$ where ρ is the density of visual elements and l_{eye} is the diameter of the eye. The density of visual elements is a decreasing function of the size of the eye: $\rho \propto l_{\text{eye}}^{-d}$ with $d \approx 0.5$ (Dunbrack & Ware 1987). Assuming that the size of the eye and the preferred size of the prey scales with the length of the predator gives the number of visual elements as

$$n \propto l^{4-d} R^{-2}.$$

The largest distance R that a predator can discern a prey of size (length) l_{prey} is when the apparent contrast (the difference between the visual imprint of the prey and the background) of the prey C_a equals the contrast threshold that the predator can distinguish C_t . Apparent contrast of the prey declines away from the

inherent contrast $C_0 = 0.3$ as:

$$C_a = C_0 e^{-\alpha R}.$$

Where $\alpha = 0.001 \text{ cm}^{-1}$ is the attenuation of light by the water. The contrast threshold is a declining function of the number of visual elements n involved in discerning the object:

$$C_t = C_{t.\min} + 1/n$$

where $C_{t.\min} = 0.15$ is the minimum contrast threshold for vision which depends on the ambient light. This semi-heuristic relationship is known as “Ricco’s law” (Northmore et al. 1978). The maximum distance where the prey can be perceived is when the apparent contrast reaches the contrast threshold, $C_a = C_t$:

$$C_0 e^{-\alpha R} = C_{t.\min} + KR^2 l^{d-4}$$

where $K = 0.025 \text{ cm}^{1.5}$ is a constant which characterizes the sensitivity of the eye. It is not possible to isolate R from the expression above. However, two limiting cases can be derived: 1) the “clear-water” limit is when the visual range is limited by the resolution of the eye, i.e. where $e^{-\alpha R} \approx 1$ and $C_0 \gg C_{t.\min}$:

$$R \approx \sqrt{C_0/K} l^{2-d/2}$$

In this case the maximum visual range increases with $l^{2-2/d} \approx l^{1.75}$ for $d = 0.5$. 2)

The “turbid-water” limit is when the visual range is limited by the sensitivity (the minimum contrast threshold) of a visual element, when $C_{t.min} \gg KR^2l^{4-d}$:

$$R \approx \frac{\ln C_o - \ln C_{t.min}}{\alpha}$$

In this limit the size of the predator does not play a role and the minimum contrast threshold essentially limits the visual range. The visual range decreases if the light in the water is limited (lower minimum contrast threshold $C_{t.min}$) or the turbidity α is increased. The prediction of this limit has been subject of more elaborate models (Aksnes & Utne 1997).

1040

1041

Sidebar 2 Life-history optimization of offspring size

The optimal life history strategy in terms of offspring size and adult size is the strategy that maximizes lifetime reproductive output (Charnov 1993). In optimal life history theory lifetime reproductive output is determined by the mortality and the available energy as functions of size or age. Here we determine the offspring size which maximizes lifetime reproductive out using arguments from Christiansen & Fenchel (1979) and Andersen *et al.* (2008).

The available energy can be assumed from metabolic scaling arguments to be $H(w) = Aw^n$ where the usual metabolic assumption is $n = 3/4$ (West et al. 1997). Consumption results in a mortality on their prey of $\mu(w) = \alpha w^{n-1}$ where α is a dimensionless constant relating consumption and mortality (Andersen & Beyer 2006). For simplicity we assume determinate growth where a juvenile uses all acquired energy for growth and a mature individual of size W uses all energy for reproduction; however the central results are valid for indeterminate growth as well (Andersen et al. 2008). The lifetime reproductive output (expected number of offspring during life) is:

$$R_0 = \frac{\epsilon}{2} P_{w_0 \rightarrow W} \frac{H(W)}{w_0 \mu(W)}$$

where ϵ is the reproductive efficiency, $1/2$ assumes an even sex ratio, $H(W)$ is the adult rate of reproduction (mass per time), $1/\mu(W)$ is the expected adult lifespan, $1/w_0$ is to convert from units of mass to number of offspring, and the probability

to survive from offspring size w_0 to adult size W is:

$$P_{w_0 \rightarrow W} = \exp \left[- \int_{w_0}^W \frac{\mu(w)}{H(w)} dw \right]$$

Inserting the metabolic assumptions, $H(w) = Aw^n$ and $\mu(w) = \alpha Aw^{n-1}$ yields a lifetime reproductive output of:

$$R_0 = \frac{\epsilon}{2\alpha} \left(\frac{W}{w_0} \right)^{1-\alpha}$$

Three conclusions can be drawn from this result:

- 1) If $R_0 < 1$ each female produces less than a single offspring throughout life yielding an unsustainable population. This happens when $\alpha > 1$ and it can be concluded that $\alpha < 1$.
- 2) Lifetime reproductive output only depends on the ratio between adult size and offspring size. The absolute values of the two sizes do not matter.
- 3) The larger the ratio between adult and offspring size, the higher the fitness. Organisms will therefore strive to maximize this ratio under the constraints of other external factors (Neuheimer et al.).

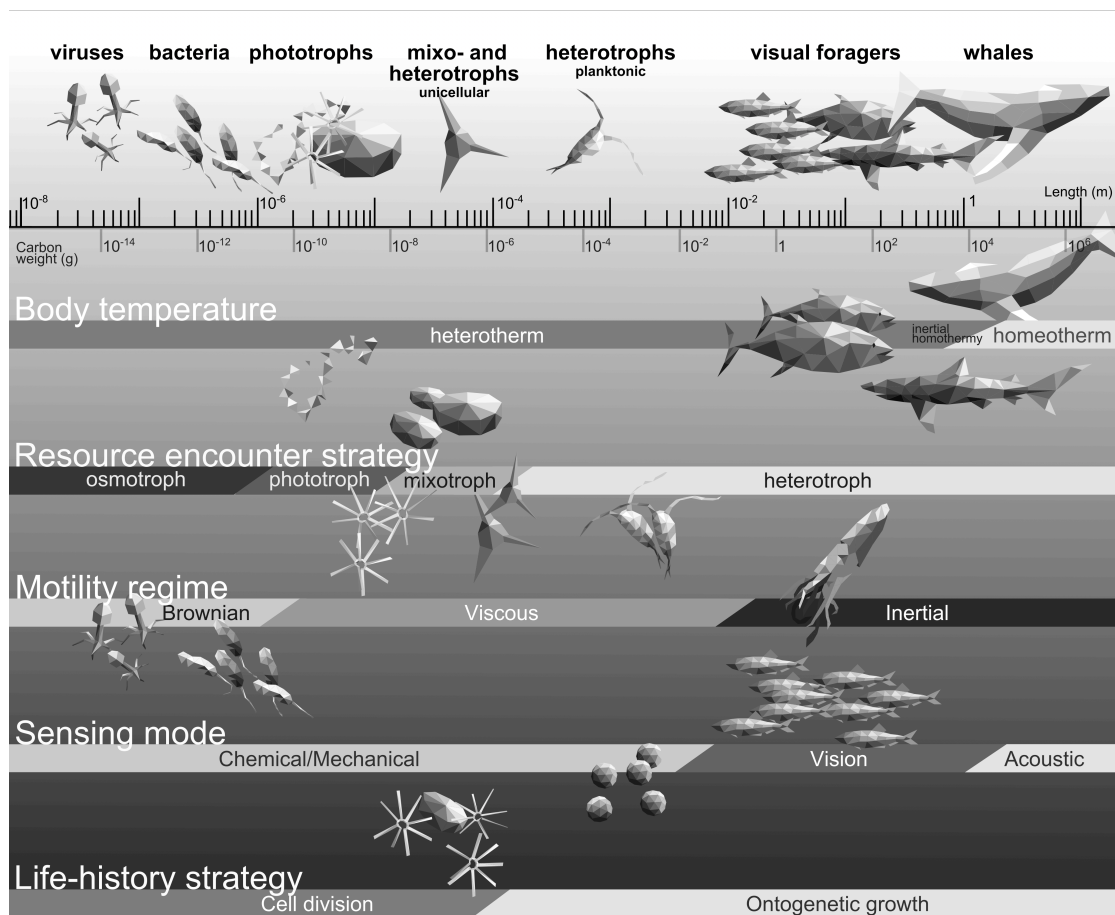
The results do not depend on the value of the metabolic exponent n as long as $n < 1$. This argument ignored the maintenance metabolism and indeterminate growth to simplify the mathematical derivation, but both of these effects can be

accounted for (Andersen et al. 2008).

1042

1043

1044 **Figures**



1047 Figure 1. The five aspects of pelagic marine life examined here (body
 1048 temperature, resource encounter strategy, motility regime, sensing mode and
 1049 life-history strategy) are illustrated with horizontal bars with the characteristic
 1050 transitions indicated by changes in gray-scale. The transitions are explained
 1051 throughout the text. The drawings in the top row illustrate the seven realms of
 1052 life: viruses, osmo-heterotrophic bacteria, unicellular phototrophs, unicellular
 1053 mixo- and heterotrophs, planktonic multi-cellular heterotrophs, visually foraging
 1054 poikilotherms (teleosts, cephalopods and sharks) and homeothermic animals
 1055 (whales).

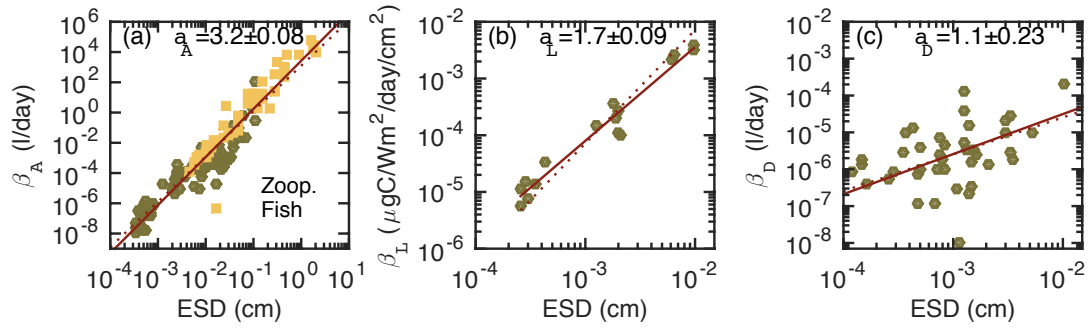
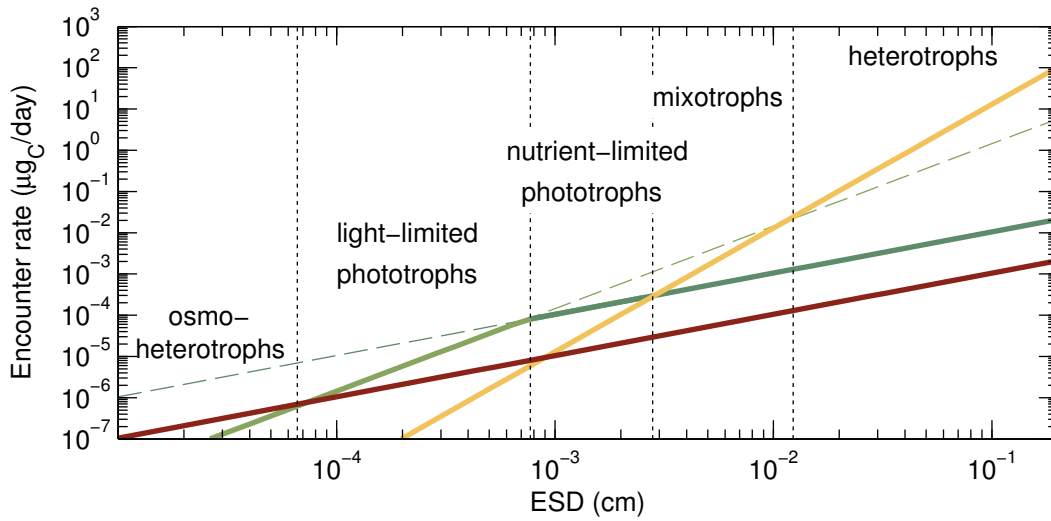


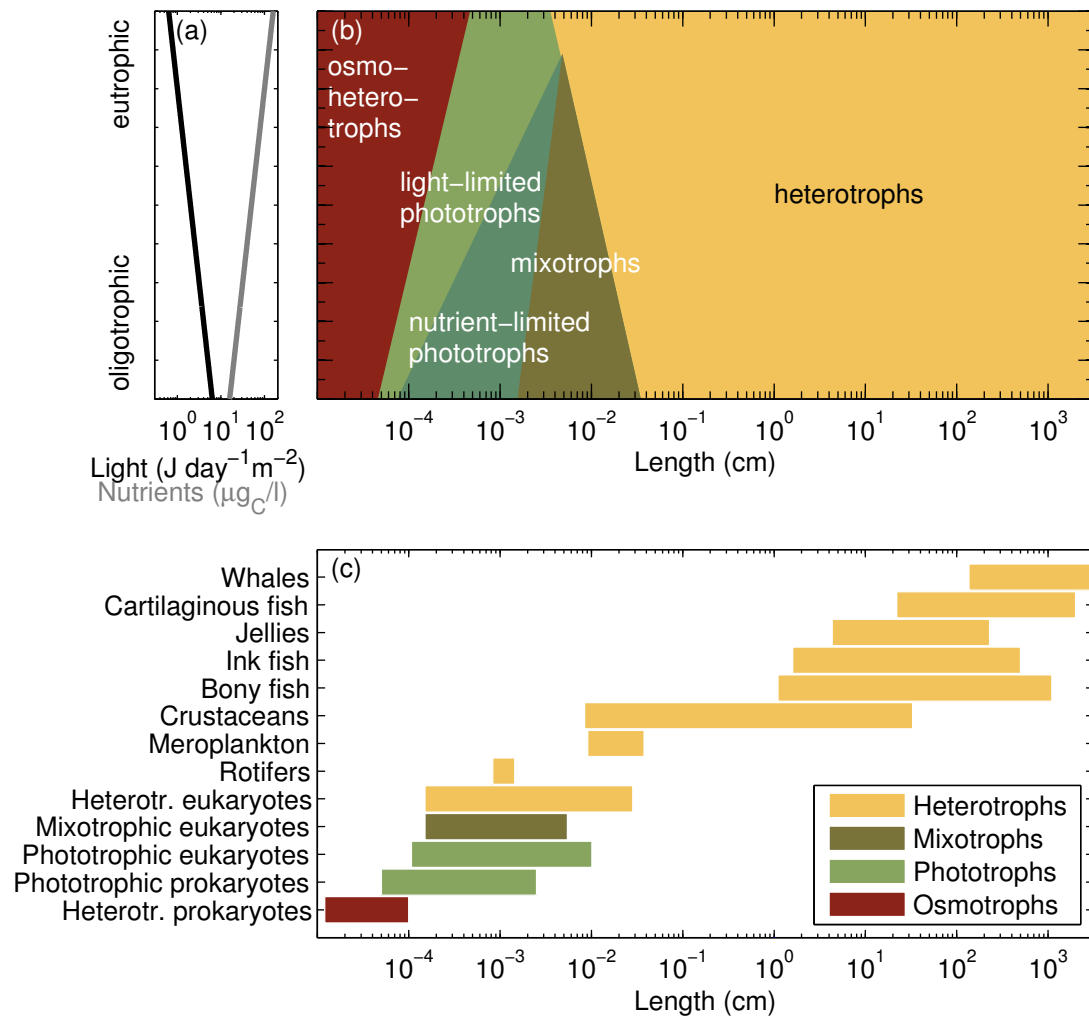
Figure 2. Clearance rate vs. weight for organisms performing active predation, photosynthesis and diffusive feeding on phosphorous. The solid lines are fits to data with exponent given in each panel. The dashed lines are fits with theoretical exponents 3, 2 and 1 for panel a, b and c respectively (Table S1.2). (a) Clearance rate β_A for active predation by zooplankton (circles) and fish (squares) from Kiørboe (2011). (b) Clearance rate β_L (affinity) for carbon uptake from a series of experiments with diatoms under identical conditions (Taguchi 1976). Data compilations covering a wider range of sizes and phytoplankton groups give a similar exponent but a larger scatter (Schwaderer et al. 2011). (c) Clearance rate β_D (affinity) for diffusive feeding on dissolved phosphate from Tambi et al. (2009) and Edwards et al. (2012).

1070



1071

1072 Figure 3. Encounter rates as a function of size for four different resource
 1073 acquisition mechanisms and resource types: diffusive uptake of dissolved
 1074 organic matter scaling as l^1 (dark red), uptake of carbon through photosynthesis
 1075 scaling as l^2 (light green), diffusive uptake of dissolved inorganic nutrients (dark
 1076 green), and active encounter of prey organisms scaling as l^3 (yellow). The
 1077 combined uptake of carbon and nutrients by phototrophs is limited by Liebig's
 1078 law and shown with solid green lines; light green for light-limited conditions and
 1079 dark green for nutrient-limited conditions. The concentration of dissolved
 1080 organic matter is $C_{\text{DOM}} = 5 \mu\text{g}_\text{C}/\text{l}$; inorganic nutrients is $C_N = 4 \mu\text{molN}/\text{l}$
 1081 (corresponding to $50 \mu\text{g}_\text{C}/\text{l}^{-1}$), the light intensity at depth is $C_L = 2 \text{ W m}^{-2}$ and the
 1082 concentration of suitable prey organisms is $C_P = 10 \mu\text{g}_\text{C}/\text{l}$.

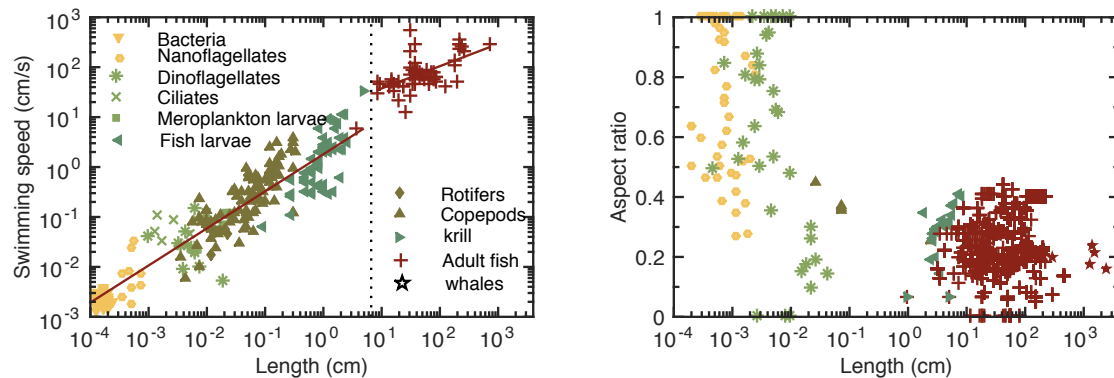


1083
1084

1085 Figure 4. Trophic strategy as a function of size: osmo-heterotrophs (dark red),
1086 phototrophs (green), mixotrophs (army green) and heterotrophs (yellow). (a)
1087 Prescribed variation of nutrient and light conditions from oligotrophic to
1088 eutrophic conditions. (b) Strategy that yields the highest resource encounter rate
1089 as a function of size (x-direction) and resource condition (y-direction) changing
1090 between oligotrophic (high light, low nutrients) to eutrophic conditions (low
1091 light, high nutrients). (c) Trophic strategy of 3020 marine organisms as a
1092 function of length. Ciliates and flagellates have been categorized as phototrophs,
1093 mixotrophs or heterotrophs depending on the trophic strategy for the specific
1094 species (Appendix S2 in Supporting Information). The groupings are whales

1095 (Cetacea only, i.e. dolphins and whales), cartilaginous fish (Elasmobranchii;
1096 sharks and rays), teleosts (Osteichthyes), Cephalopoda (“ink fish”),
1097 meroplanktonic larvae (i.e. planktonic larvae whose adult stages are benthic),
1098 jellies (Cnidaria, Ctenophora), rotifers (Rotifera), crustaceans (incl. copepods),
1099 and unicellular eukaryotes or prokaryotes.
1100

1101

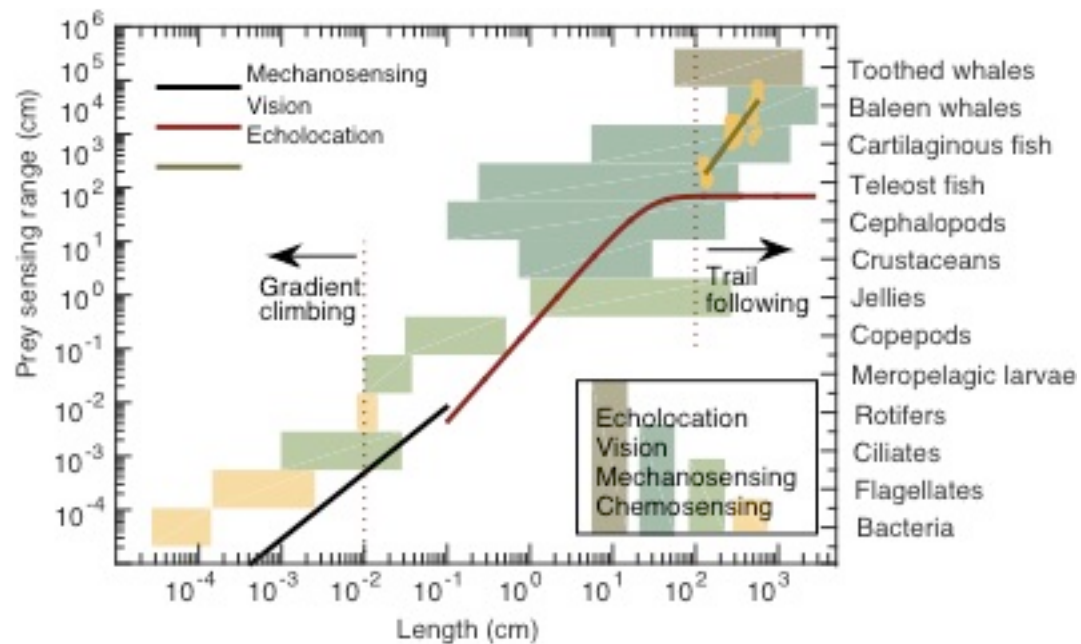


1102

1103 Figure 5. Swimming speeds and body aspect ratio vs. body length. Length is
1104 measured as ESD for planktonic organisms and as longest length for fish larvae,
1105 krill, fish and whales. (a) Swimming speed: data for zooplankton (including fish
1106 larvae) from Kiørboe (2011); fish data (cruising speed) from Sambilay Jr. (1990).
1107 The lines are power law fits (Table 1). The split between the two data sets was
1108 determined as the size that gave the lowest total residual of the fits. The
1109 crossover size at 6.6 cm corresponds to a Reynolds number around 1000. (b)
1110 Aspect ratio as a function of length for motile marine organisms. Data contain
1111 nanoflagellates and dinoflagellates (Throndsen et al. 2003, Tomas 1997),
1112 copepods (Kiørboe et al. 2010), krill (Watkins & Brierley 2002), fish larvae (Ara
1113 et al. 2013, Morioka et al. 2013, Moser et al. 1986, Oka & Higashiji 2012) and
1114 adult fish (Froese & Pauly 2013).

1115

1116



1117

1118

1119

1120 Figure 6. . Senses vs. size. Left axis and lines: Estimated range for sensing a prey a
 1121 factor 10 shorter than a predator. (see Sidebar 1 for details). Echolocation range
 1122 determined from tank and field measurements of tooth whales of different size
 1123 (circles; Table S3.2). The line is fitted with exponent $17/8$ (table 1). The vertical
 1124 lines are estimates of limits of chemotaxis strategies; see text for details. Right
 1125 axis and bars: Senses used for detecting prey grouped according to size and
 1126 organismal group (Table S3.1).

1127

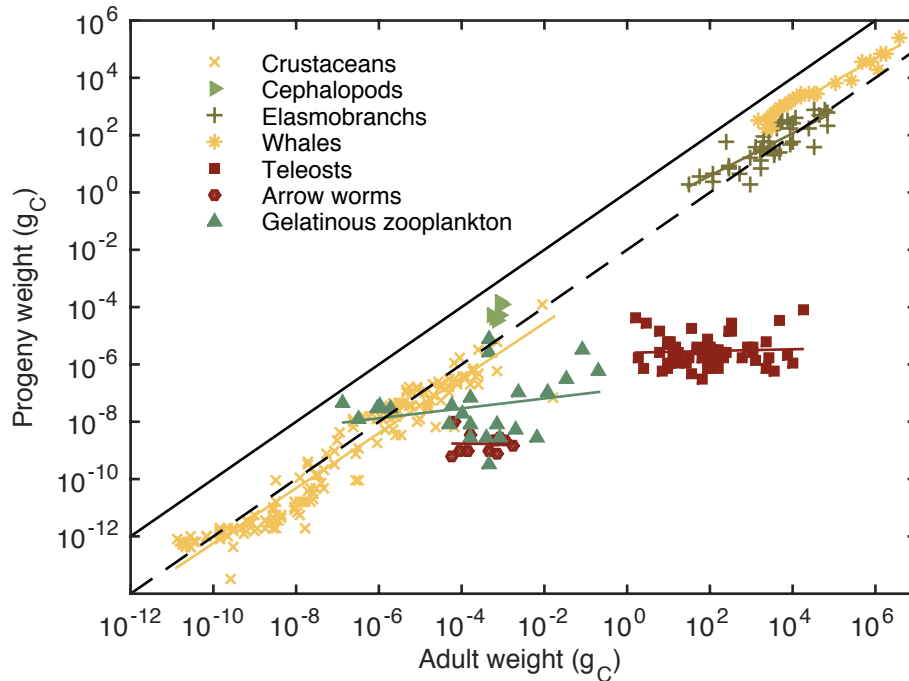


Figure 7. Weights of adults and progeny for metazoans grouped by species of similar taxonomy. Estimates of mean adult and progeny size were compiled from the literature, with “adult” defined as individuals that had reached maturity and “progeny” the smallest size at which offspring are independent of the parent (Appendix S4). Original data included measures of volume, length, wet weight, dry weight and carbon dry weight. All were converted to carbon dry weight using either species-specific or, if unavailable, group-specific conversion factors from the literature. The solid line is a 1:1 progeny:adult size ratio and the dashed line is a 1:100 progeny:adult size ratio. Life forms following this line (whales, cartilaginous fish and crustaceans) follow the “fixed-ratio” strategy, while life forms with constant progeny size (most notably teleost fish) follow the “small-eggs” strategy.